

Asymmetric phase diagram of mixed $\text{CuInP}_2(\text{S}_x\text{Se}_{1-x})_6$ crystalsJ. Macutkevicius,^{1,*} J. Banys,² R. Grigalaitis,² and Yu. Vysochanskii³¹Semiconductor Physics Institute, A. Gostauto 11, 2600 Vilnius, Lithuania²Faculty of Physics, Vilnius University, Sauletekio 9, Vilnius LT-10222, Lithuania³Institute of Solid State Physics and Chemistry, Uzhgorod University, Voloshyn 54, Uzhgorod 88000, Ukraine

(Received 28 December 2007; published 1 August 2008)

Mixed $\text{CuInP}_2(\text{S}_x\text{Se}_{1-x})_6$ crystals were investigated by broadband dielectric spectroscopy (20 Hz–3 GHz). The complete phase diagram has been obtained. The phase diagram of investigated crystals is strongly asymmetric—the decreasing of ferroelectric phase-transition temperatures in $\text{CuInP}_2(\text{S}_x\text{Se}_{1-x})_6$ is much more flat with small admixture of sulfur than with small admixture of selenium. In the middle part of the phase diagram ($x=0.4$ – 0.9) the dipolar glass phase has been observed. In boundary region between ferroelectric order and dipolar glass disorder with small amount of sulfur ($x=0.2$ – 0.25) at low temperatures, the nonergodic relaxor phase appears. The phase diagram was discussed in terms of random bonds and random fields.

DOI: 10.1103/PhysRevB.78.064101

PACS number(s): 77.80.–e, 77.22.Gm

I. INTRODUCTION

Solid systems present many interesting types of phase transitions, with ferro, antiferro, or modulated long-range order at lower temperatures. Disordered cooperative systems have also attracted a lot of attention. Nonergodic relaxor, dipolar glass phases, or coexistence of ferroelectric and dipolar glass phases can appear in disordered systems at low temperatures. The nature of these phases continues to generate considerable experimental and theoretical interest.

CuInP_2S_6 crystals represent an unusual example of an anticollinear two-sublattice ferroelectric system.^{1–4} Here the first-order phase transition of the order-disorder type from the paraelectric to the ferroelectric phase is realized ($T_c=315$ K). The symmetry reduction at the phase transition ($C2/c \rightarrow Cc$) occurs due to ordering in the copper sublattice and displacement of cations from the centrosymmetric positions in the indium sublattice. The spontaneous polarization arising at the phase transition to the ferroelectric phase is perpendicular to the layer planes. These thiophosphates consist of lamellae defined by a sulfur framework in which the metal cations and P-P pairs fill the octahedral voids; within a layer, the Cu, In, and P-P form triangular patterns.^{1–3} The cation off centering, 1.6 Å for Cu^I and 0.2 Å for In^{III} , may be attributed to a second-order Jahn-Teller instability associated with the d^{10} electronic configuration. The lamellar matrix absorbs the structural deformations via the flexible P_2S_6 groups while restricting the cations to antiparallel displacements that minimize the energy costs of dipole ordering. Each Cu ion can occupy two different positions. The Cu, In, and P-P form triangular patterns within the layer. Relaxational rather than resonant behavior is indicated by the temperature dependence of the spectral characteristics, which is in agreement with x-ray investigations. It was suggested that a coupling between P_2S_6 deformation modes and Cu^I vibrations enables the copper ion hopping motions that lead to the loss of polarity and the onset of ionic conductivity in this material at higher temperatures.⁴ The investigation of ionic conductivity in CuInP_2S_6 (Refs. 5 and 6) has showed that σ_{dc} follows the Arrhenius law with the activation energy $E_A=0.73$ eV (Ref. 5) and more detailed investigations showed $E_A=0.635$ eV.⁶

The results of dielectric investigations of $\text{CuInP}_2\text{Se}_6$ showed two phase transitions: a second-order one at $T_i=248$ K and a first-order transition at $T_c=236$ K.⁷ The results followed to the conclusion that an incommensurate phase occurs between T_i and T_c . However, the calorimetric investigations showed only a broad phase transition between 220 and 240 K in this compound.⁸ More accurate broadband dielectric investigations showed only nearly second-order phase transition at $T_c=226$ K.⁹ From a single-crystal x-ray diffraction study follows that the high- and low-temperature structures of $\text{CuInP}_2\text{Se}_6$ (trigonal space groups $P\bar{3}1c$ and $P31c$, respectively) are very similar to those of CuInP_2S_6 in the paraelectric and ferroelectric phases, with the Cu^I off-centering shift being smaller in the former than in the latter.^{3,8} There the thermal evolution of the cell parameters of $\text{CuInP}_2\text{Se}_6$ was obtained by full profile fits to the x-ray diffractograms. Both cell parameters a and c slightly decrease on cooling, and a parameter shows a local minimum at $T=226$ K. This behavior is quite different from the anomalous increases found in the cell parameters of CuInP_2S_6 when heating through the transition.^{1,3}

The important feature of selenides is the higher covalence degree of their bonds. Evidently, for this reason the copper ion sites in the low-temperature phase of $\text{CuInP}_2\text{Se}_6$ are displaced only by 1.17 Å (Ref. 8) from the middle of the structure layers in comparison with the corresponding displacement of 1.6 Å for CuInP_2S_6 .¹ These facts enable us to assume that the potential relief for copper ions in $\text{CuInP}_2\text{Se}_6$ is shallower than for its sulfide analog.¹⁰ Presumably, for this reason the structural phase transition in the selenide compound is observed at lower temperature than for the sulfide compound. Preliminary dielectric investigations of $\text{CuInP}_2(\text{S}_x\text{Se}_{1-x})_6$ crystals are presented in Refs. 11 and 12. The data in Ref. 11 are measured only at frequency of 10 kHz and the paper¹² contains data only on one compound— $\text{CuInP}_2(\text{S}_{0.7}\text{Se}_{0.3})_6$.

The aim of this paper is to investigate phase diagram of mixed $\text{CuInP}_2(\text{S}_x\text{Se}_{1-x})_6$ crystals via broadband dielectric spectroscopy. We showed that in mixed crystals with the increasing amount of impurities two smearing of ferroelectric phase-transition scenarios are possible: ferroelectric–

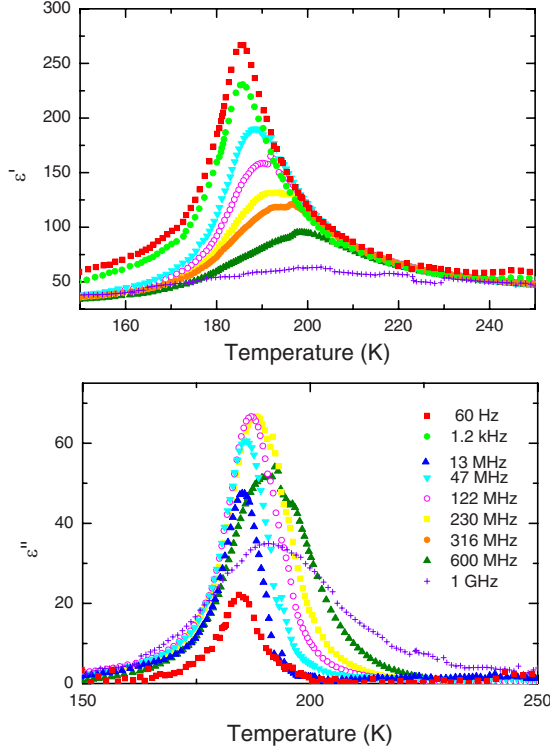


FIG. 1. (Color online) Temperature dependence of the complex dielectric permittivity of $\text{CuInP}_2(\text{S}_{0.1}\text{Se}_{0.9})_6$ crystals measured at several frequencies.

inhomogeneous ferroelectric–dipolar glass or ferroelectric–relaxor–dipolar glass.

II. EXPERIMENT

Crystals of $\text{CuInP}_2(\text{S}_x\text{Se}_{1-x})_6$ were grown by Bridgman method. For the dielectric spectroscopy the platelike crystals were used. All measurements were performed in direction perpendicular to the layers. The complex dielectric permittivity ϵ^* was measured using the HP4284A capacitance bridge in the frequency range 20 Hz–1 MHz. In the frequency region from 1 MHz to 3 GHz measurements were performed by a coaxial dielectric spectrometer with vector network analyzer Agilent 8714ET. All measurements have been performed on cooling with controlled temperature rate of 0.25 K/min. Silver paste has been used for contacting.

III. RESULTS AND DISCUSSION

A. Influence of small amount of sulfur to phase-transition dynamics in $\text{CuInP}_2\text{Se}_6$ crystals

A small amount of admixture can significantly change properties of ferroelectrics. In mixed $\text{CuInP}_2(\text{S}_x\text{Se}_{1-x})_6$ crystals with $x \leq 0.1$ the ferroelectric phase transition is observed (Fig. 1). Here the dielectric permittivity maximum temperature (T_m) is frequency dependent only at higher frequencies (above 1 MHz). The phase-transition temperature can be defined by T_m at low frequencies (below 1 MHz).

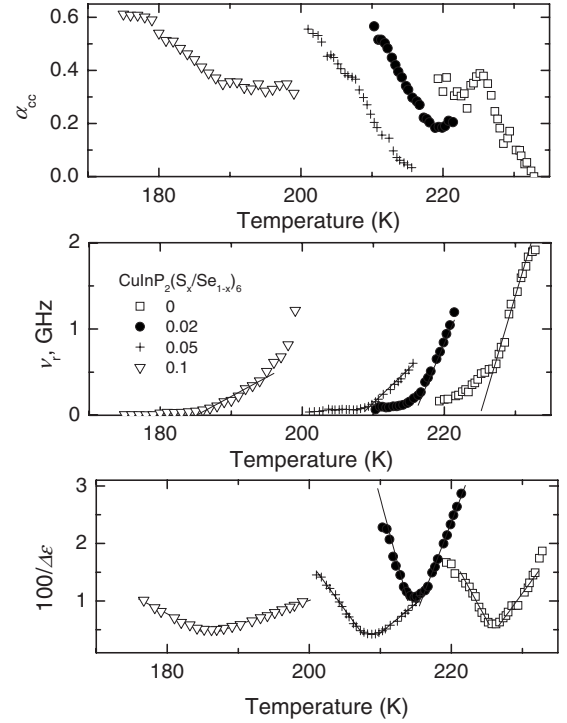


FIG. 2. Temperature dependence of the Cole-Cole parameters of complex dielectric permittivity for the $\text{CuInP}_2(\text{S}_x\text{Se}_{1-x})_6$ crystals with $x \leq 0.1$. The ν_r lines were obtained from fit with Eq. (3) and the $1/\Delta\epsilon$ lines were obtained from Curie-Weiss fit. The data for $\text{CuInP}_2\text{Se}_6$ are from Ref. 9.

More information about the phase-transition dynamics can be obtained by analysis of the dielectric dispersion with the Cole-Cole formula,

$$\epsilon^*(\nu) = \epsilon_\infty + \frac{\Delta\epsilon}{1 + (i\omega\tau_{CC})^{1-\alpha_{CC}}}, \quad (1)$$

where $\Delta\epsilon$ represents dielectric strength of the relaxation, τ_{CC} is the mean Cole-Cole relaxation time, ϵ_∞ represents the contribution of all polar phonons and electronic polarization to the dielectric permittivity, and α_{CC} is the Cole-Cole relaxation-time distribution parameter; when $\alpha_{CC}=0$, Eq. (1) reduces to the Debye formula. Obtained parameters are presented in Fig. 2. The Cole-Cole parameters of all presented compounds show the similar behavior: the Cole-Cole distribution parameter α_{CC} strongly increases on cooling, reciprocal dielectric strength $1/\Delta\epsilon$ exhibits a minimum at ferroelectric phase-transition temperature, and the relaxational soft-mode frequency $\nu_r=1/(2\pi\tau_{CC})$ slows down on cooling in the paraelectric phase. The temperature dependence of the dielectric strength $\Delta\epsilon$ was fitted with the Curie-Weiss law (Fig. 2),

$$\Delta\epsilon = C_{p,f}/(|T - T_C|), \quad (2)$$

where $C_{p,f}$ is the Curie-Weiss constant and T_C is the Curie-Weiss temperature. The temperature dependence of relaxational soft-mode frequency ν_r in paraelectric phase was fitted with the equation

TABLE I. Parameters of phase-transition dynamics of $\text{CuInP}_2\text{Se}_6$ crystals with small admixture of sulfur ($x \leq 0.1$).

Compound	C_p (K)	C_p/C_f	A (MHz/K)	T_C (K)
$\text{CuInP}_2\text{Se}_6$ ^a	591.7	1.33	271.9	225
$\text{CuInP}_2(\text{Se}_{0.98}\text{S}_{0.02})_6$	309.6	1.43	193.4	215.7
$\text{CuInP}_2(\text{Se}_{0.95}\text{S}_{0.05})_6$	980.3	1.66	79.3	208.2
$\text{CuInP}_2(\text{Se}_{0.9}\text{S}_{0.1})_6$	2380.9	1.52	44.4	185

^aFrom Ref. 9.

$$\nu_r = A(T - T_C), \quad (3)$$

where A is a constant. Obtained parameters are presented in Table I. The phase-transition temperature T_C in mixed crystals strongly decreases from 225 to 185 K. For all the compounds the C_p/C_f ratio is about 1.5, for the second-order phase transitions this ratio must be 2, and for the first-order one higher than 2. The assumption was made that in these crystals between paraelectric and ferroelectric phase an additional incommensurate phase exists.¹¹ However, in all mixed $\text{CuInP}_2(\text{S}_x\text{Se}_{1-x})_6$ crystals with $x \leq 0.1$ no anomaly above the main (ferroelectric) phase transition was observed (Fig. 1).

Below the ferroelectric phase-transition temperature the dielectric dispersion is broad and part of it appears in the low-frequency region (Fig. 1). This part is caused by ferroelectric domain dynamics. Therefore, the contribution of ferroelectric domain dynamics effectively raises the dielectric strength $\Delta\epsilon$ in the ferroelectric phase and C_f constant.

B. Nonergodic relaxor phase in mixed $\text{CuInP}_2(\text{S}_x\text{Se}_{1-x})_6$ crystals

Recently, the relaxorlike behavior as an embryo of the glass state is proposed in the antiferroelectric-glass phase boundary region of $\text{Rb}_{1-x}(\text{ND}_4)_x\text{D}_2\text{PO}_4$ (DRADP) crystal family.¹³ Here it is showed that the growth of glass ordering is in quite a different pattern from that of the ferroelectric-glass phase boundary region. In this section we shall presented two very similar $\text{CuInP}_2(\text{S}_x\text{Se}_{1-x})_6$ compounds ($x = 0.2$ and $x = 0.25$), which exhibit peculiar dielectric behavior. Each composition shows just one maximum in $\epsilon'(T)$ and $\epsilon''(T)$ in the range of 110 and 145 K at frequency of 10 kHz.¹¹

The temperature dependences of the complex dielectric permittivity ϵ^* at various frequencies of these crystals show typical relaxor behavior. As an example, dielectric permittivity of $\text{CuInP}_2(\text{Se}_{0.75}\text{S}_{0.25})_6$ crystal is shown in Fig. 3. There is a broad peak in the real part of dielectric permittivity that is observed. With frequency T_m the magnitude of the peak increases in the whole frequency range. There is a strong dielectric dispersion in a radio frequency region around and below T_m at 1 kHz. The value of T_m (the temperature of the maximum of losses) is much lower than that of T_m at the same frequency. The position of the maximum of dielectric permittivity is strongly frequency dependent; no certain static dielectric permittivity can be obtained below and

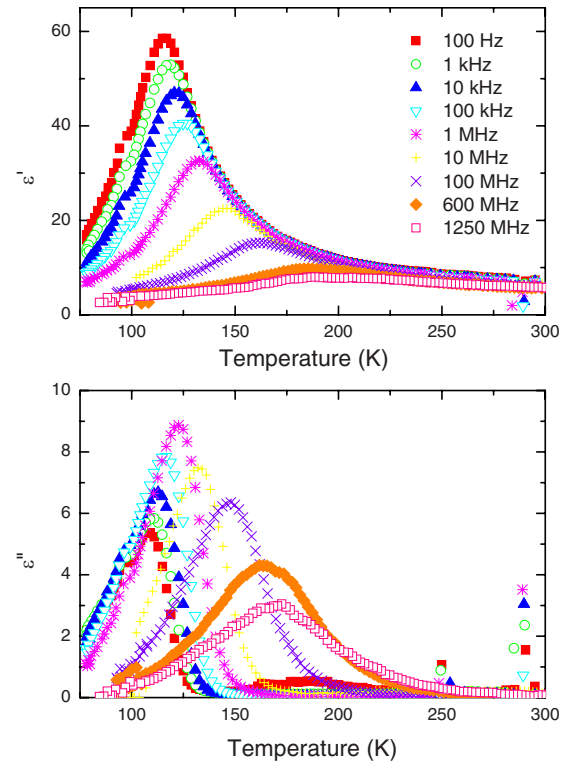


FIG. 3. (Color online) Temperature dependence of the complex dielectric permittivity of $\text{CuInP}_2(\text{S}_{0.25}\text{Se}_{0.75})_6$ crystals measured at several frequencies.

around dielectric permittivity maximum temperature T_m at 1 kHz. Such behavior can be described by the Vogel-Fulcher relationship,

$$\nu = \nu_0 \exp \frac{-E_f}{k(T_m - T_{0f})}, \quad (4)$$

where k is the Boltzmann constant and E_f , ν_0 , and T_{0f} are parameters of this equation. Obtained parameters are presented in Table II.

The dielectric dispersion of $\text{CuInP}_2(\text{Se}_{0.75}\text{S}_{0.25})_6$ crystals shows strong temperature dependence (Fig. 4): at higher temperatures the dielectric dispersion is only in $10^7 - 10^{10}$ Hz region, and on cooling the dielectric dispersion becomes broader and more asymmetric. Strongly asymmetric and very broad dielectric dispersion is observed below dielectric permittivity maximum temperature T_m at 1 kHz. The Cole-Cole formula [Eq. (1)] can describe such dielectric dispersion only at higher temperatures due to predefined sym-

TABLE II. Parameters of the Vogel-Fulcher fit of the T_m dependence of frequency for $\text{CuInP}_2(\text{S}_x\text{Se}_{1-x})_6$ crystals with $0.2 \leq x \leq 0.25$.

Compound	ν_0 (GHz)	T_{0f} (K)	E_f/k (K)
$\text{CuInP}_2(\text{Se}_{0.75}\text{S}_{0.25})_6$	38.34	96.8	370
$\text{CuInP}_2(\text{Se}_{0.8}\text{S}_{0.2})_6$	10.96	134.5	150

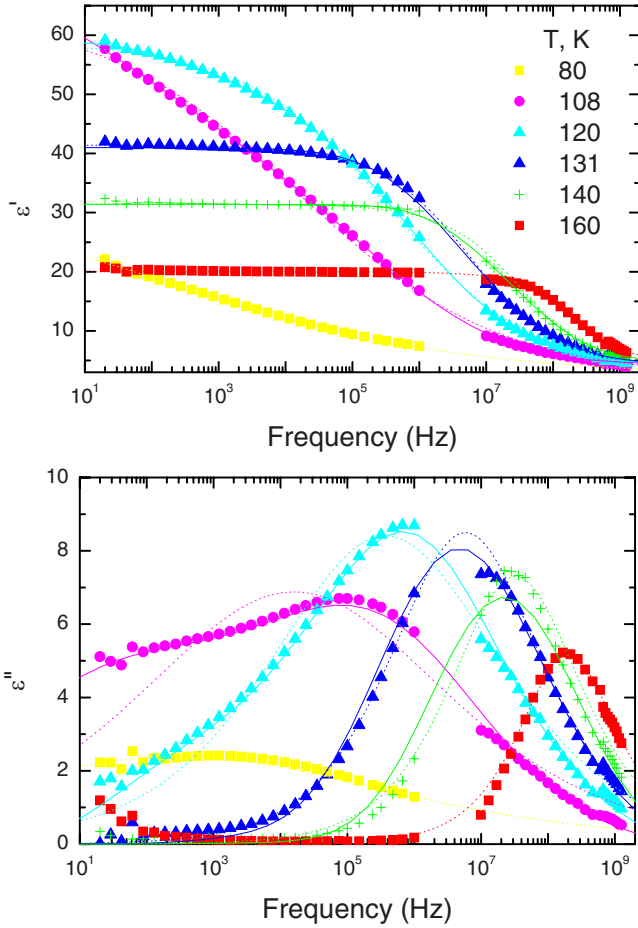


FIG. 4. (Color online) Frequency dependence of the complex dielectric permittivity of $\text{CuInP}_2(\text{S}_{0.25}\text{Se}_{0.75})_6$ crystals at several temperatures. Lines are results of fits with distributions of relaxation times (solid) and of Cole-Cole fit (dot).

metric shape of the distribution of the relaxation times. This is clearly visible in Fig. 4, where the Cole-Cole fit is shown as dotted line. Not only Cole-Cole formula but also other very well-known predefined dielectric dispersion formulas, such as Havriliak-Negami and Cole-Davidson, cannot adequately describe the dielectric dispersion of the presented crystals. More general approach must be used for determination of the broad continuous distribution function of relaxation times $f(\tau)$ by solving Fredholm integral equations,

$$\epsilon'(\omega) = \epsilon_\infty + \Delta\epsilon \int_{-\infty}^{\infty} \frac{f(\tau)d(\ln \tau)}{1 + \omega^2\tau^2}, \quad (5a)$$

$$\epsilon''(\omega) = \Delta\epsilon \int_{-\infty}^{\infty} \frac{\omega\tau f(\tau)d(\ln \tau)}{1 + \omega^2\tau^2}, \quad (5b)$$

with the normalization condition

$$\int_{-\infty}^{\infty} f(\tau)d(\ln \tau) = 1. \quad (6)$$

The most general method for the solution is the Tikhonov regularization^{14,15} method. The calculated distribution of re-

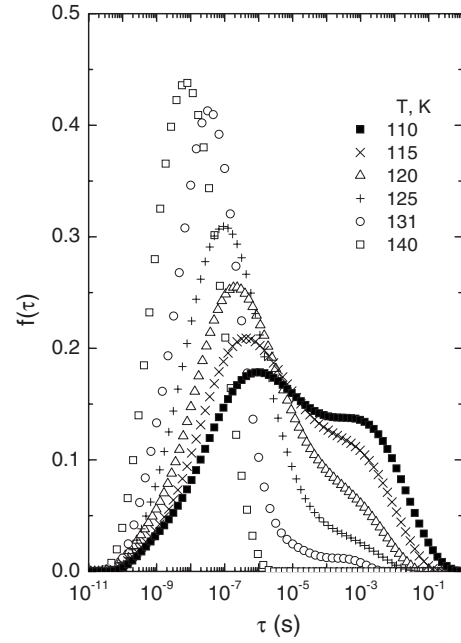


FIG. 5. Relaxation-time distribution for $\text{CuInP}_2(\text{S}_{0.25}\text{Se}_{0.75})_6$ crystals at various temperatures.

laxation times of $\text{CuInP}_2(\text{S}_{0.25}\text{Se}_{0.75})_6$ crystals is presented in Fig. 5. The symmetric and narrow distribution is observed only at higher temperature $T \gg T_m$ (at 1 kHz); on cooling the distribution becomes broader and more asymmetric so that below T_m (at 1 kHz) second maximum appears. Such behavior of distribution of relaxation times has been already observed in a very well-known relaxors: $\text{Pb}(\text{Mg}_{1/3}\text{Nb}_{2/3})\text{O}_3$ (PMN),¹⁶ $\text{Pb}(\text{Mg}_{1/3}\text{Nb}_{2/3})\text{O}_3 - \text{Pb}(\text{Zn}_{1/3}\text{Nb}_{2/3})\text{O}_3 - \text{Pb}(\text{Sc}_{1/2}\text{Nb}_{1/2})\text{O}_3$ (PMN-PZN-PSN),¹⁷ $\text{Pb}(\text{Mg}_{1/3}\text{Ta}_{2/3})\text{O}_3$ (PMT),¹⁸ and $\text{Sr}_{0.61}\text{Ba}_{0.39}\text{Nb}_2\text{O}_6$ (SBN).¹⁹ From calculated distributions of relaxation times the most probable relaxation time τ_{mp} , longest relaxation time τ_{max} , and shortest relaxation time τ_{min} (the level 0.1 was chosen as sufficiently accurate) have been obtained (Fig. 6). The shortest relaxation time τ_{min} is about 0.1 ns for $\text{CuInP}_2(\text{S}_{0.25}\text{Se}_{0.75})_6$ and is about 0.01 ns for $\text{CuInP}_2(\text{S}_{0.2}\text{Se}_{0.8})_6$; it increases slowly with the increase in temperature. The longest relaxation time τ_{max} diverges according to the Vogel-Fulcher law,

$$\tau_{\text{max}} = \tau_{0\text{max}} \exp \frac{E_{\text{max}}}{k(T - T_0)}, \quad (7)$$

where T_0 is the freezing temperature, E_{max} is the activation energy of the longest relaxation times τ_{max} , and $\tau_{0\text{max}}$ is the longest relaxation time at very high temperatures. The obtained parameters are presented in Table III; however the most probable relaxation time τ_{mp} diverges with good accuracy according to the Arrhenius law,

$$\tau_{\text{mp}} = \tau_{0\text{mp}} \exp \frac{E_{\text{mp}}}{kT}, \quad (8)$$

where E_{mp} is the activation energy of the most probable relaxation times τ_{mp} and $\tau_{0\text{mp}}$ is the most probable relaxation

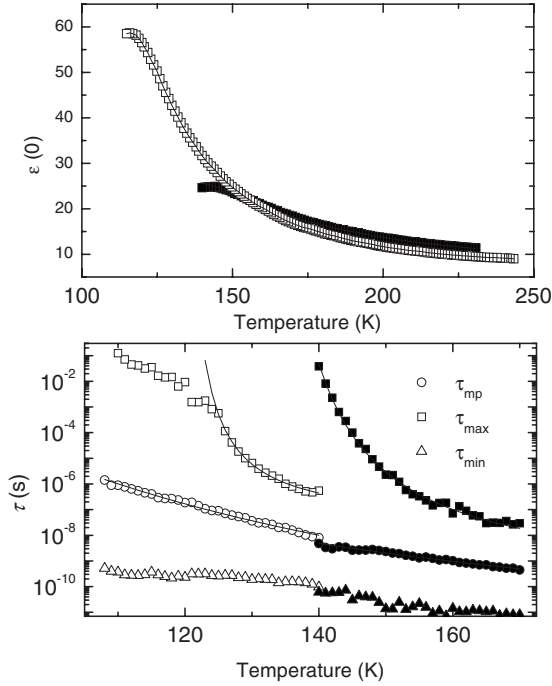


FIG. 6. Temperature dependence of the longest τ_{\max} , most probable τ_{mp} , shortest τ_{\min} relaxation times, and static dielectric permittivity $\varepsilon(0)$ in $\text{CuInP}_2(\text{S}_x\text{Se}_{1-x})_6$ crystals, with $x=0.2$ (solid points) and $x=0.25$ (open points). The $\tau(T)$ lines were obtained from Vogel-Fulcher (for longest relaxation times) and from Arrhenius (for most probable relaxation times) fits. The static dielectric permittivity $\varepsilon(0)$ lines were obtained from Eqs. (9) and (10).

time at very high temperatures. Obtained parameters are $\tau_{0\text{mp}}=4.6 \times 10^{-16}$ s and $E_{\text{mp}}/k=2365.3$ K for $\text{CuInP}_2(\text{Se}_{0.75}\text{S}_{0.25})_6$ and $\tau_{0\text{mp}}=1.2 \times 10^{-14}$ s and $E_{\text{mp}}/k=1806.3$ K for $\text{CuInP}_2(\text{Se}_{0.8}\text{S}_{0.2})_6$. Such phenomenon can be caused by a distribution of Vogel-Fulcher temperatures T_0 , where $0 \leq T_0 \leq T_0^{\max}$.^{20,21} In our case T_0^{\max} would correspond to a Vogel-Fulcher temperature of τ_{\max} and 0 is the freezing temperature of the most probable relaxation time and all shorter relaxation times. The temperature dependence of the static dielectric permittivity $\varepsilon(0)$ was fitted with spherical random-bond random field (SRBRF),

$$\varepsilon(0) = \frac{C_p(1 - q_{\text{EA}})}{kT - J(1 - q_{\text{EA}})} + \varepsilon_{\infty}, \quad (9)$$

where J is the mean coupling constant and q_{EA} is Edwards-Anderson order parameter; if $q_{\text{EA}}=0$ then this equation becomes the Curie-Weiss law. The Edwards-Anderson order

TABLE III. Parameters of the Vogel-Fulcher fit of the temperature dependencies of the longest relaxation times τ_{\max} in $\text{CuInP}_2(\text{S}_x\text{Se}_{1-x})_6$ crystals with $0.2 \leq x \leq 0.25$.

Compound	$\tau_{0\text{max}}$ (s)	T_0 (K)	E_{max}/k (K)
$\text{CuInP}_2(\text{Se}_{0.75}\text{S}_{0.25})_6$	2.52×10^{-8}	118.9	60.5
$\text{CuInP}_2(\text{Se}_{0.8}\text{S}_{0.2})_6$	1.02×10^{-10}	129.4	211.01

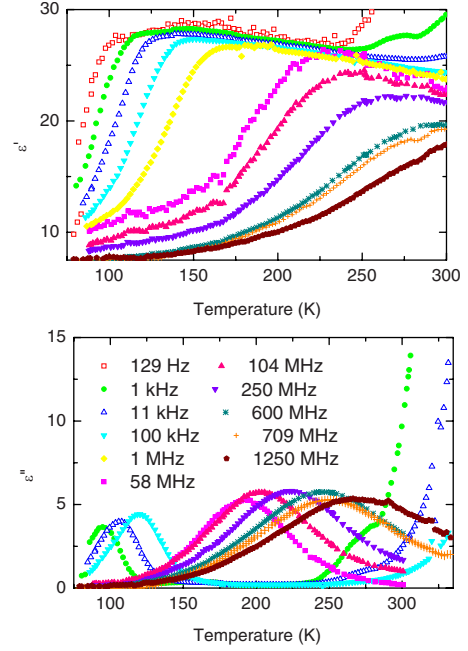


FIG. 7. (Color online) Temperature dependence of the complex dielectric permittivity of $\text{CuInP}_2(\text{S}_{0.8}\text{Se}_{0.2})_6$ crystals measured at several frequencies.

parameter q_{EA} for relaxor can be determined by equation²²

$$q_{\text{EA}} = \left(\frac{\Delta J}{kT} \right)^2 \left(q_{\text{EA}} + \frac{\Delta f}{(\Delta J)^2} \right) (1 - q_{\text{EA}})^2, \quad (10)$$

where ΔJ is the rms variance of the coupling and Δf is the variance of the random fields. We will discuss further the obtained parameters together with random-bond random-field (RBRF) parameters of other mixed crystals. We must admit that the equations of the SRBRF model describe well static dielectric properties of the presented crystals. At sulfur concentrations between $x=0.25$ and $x=0.2$, morphotropic phase boundary between the paraelectric phases $C2/c$ (characteristic for CuInP_2S_6) and $P-31c$ (characteristic for $\text{CuInP}_2\text{Se}_6$) or, respectively, ferroelectric phases Cc and $P31c$ were suggested.¹¹ These results were later confirmed by x-ray and Raman investigations.²³ Therefore, the disorder in these mixed crystals is very high, and it can be reason of relaxor nature of the presented crystals.

C. Dipolar glass phase in mixed $\text{CuInP}_2(\text{S}_x\text{Se}_{1-x})_6$ crystals

For $\text{CuInP}_2(\text{S}_x\text{Se}_{1-x})_6$ crystals with $x=0.4-0.9$ no anomaly in static dielectric permittivity indicating the polar phase transition can be detected down to the lowest temperatures. The dielectric spectra of these crystals are very similar. As an example, real and imaginary parts of the complex dielectric permittivity of $\text{CuInP}_2(\text{S}_{0.8}\text{Se}_{0.2})_6$ crystals are shown in Fig. 7 as a function of temperature at several frequencies. It is easy to see a broad dispersion of the complex dielectric permittivity starting from 260 K and extending to the lowest temperatures. The maximum of the real part of dielectric permittivity shifts to higher temperatures with increase in the frequency together with the maximum of the

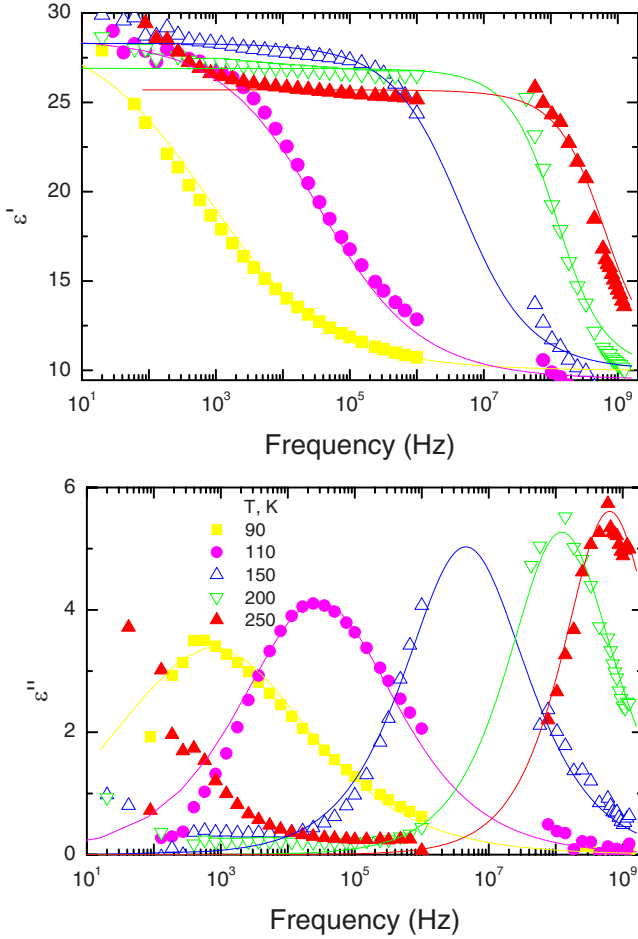


FIG. 8. (Color online) Frequency dependence of the complex dielectric permittivity of $\text{CuInP}_2(\text{S}_{0.8}\text{Se}_{0.2})_6$ crystals at several temperatures. Lines are results of Cole-Cole fits.

imaginary part and manifests typical behavior of dipolar glasses. The dielectric dispersion is symmetric of all crystals under study so that it can easily be described by the Cole-Cole formula (Fig. 8). The temperature dependence of the Cole-Cole parameters confirms typical behavior for dipolar glasses (Fig. 9): the mean Cole-Cole relaxation time diverges according to the Vogel-Fulcher law [Eq. (7)], the Cole-Cole distribution parameter α_{CC} strongly increases on cooling and reaches value 0.5 below 100 K, and the static dielectric permittivity temperature dependence has no expressed maxima. Usually such behavior is analyzed in terms of the three-dimensional (3D) RBRF Ising model of Pirc *et al.*²⁴ In terms of this model, the temperature dependence of static dielectric permittivity can be described with Eq. (9). The order parameter is defined by the two coupled self-consistent equations,²⁵

$$P = \int_{-\infty}^{\infty} \frac{dz}{(2\pi)^{0.5}} \tanh\left(\frac{\eta}{kT}\right) \exp\left(-\frac{z^2}{2}\right), \quad (11)$$

$$q_{\text{EA}} = \int_{-\infty}^{\infty} \frac{dz}{(2\pi)^{0.5}} \tanh^2\left(\frac{\eta}{kT}\right) \exp\left(-\frac{z^2}{2}\right), \quad (12)$$

where P is the polarization and

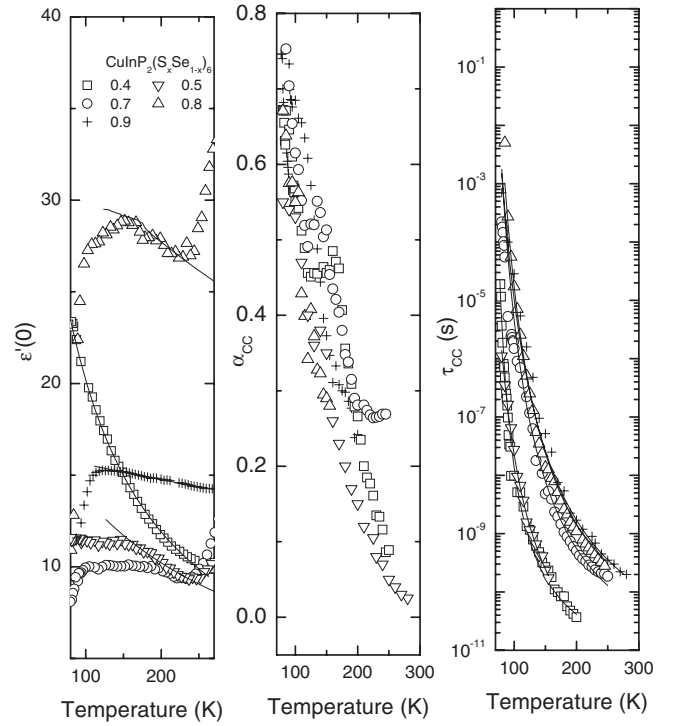


FIG. 9. Temperature dependence of the Cole-Cole parameters of complex dielectric permittivity for the $\text{CuInP}_2(\text{S}_x\text{Se}_{1-x})_6$ crystals with $0.4 \leq x \leq 0.9$. The τ lines were obtained from Vogel-Fulcher fit and the $\epsilon'(0)$ lines were obtained from 3D RBRF model fit.

$$\eta = (\Delta J^2 q_{\text{EA}} + \Delta f)^{0.5} z + JP. \quad (13)$$

Equation (9) describes good enough static dielectric properties of presented dipolar glasses and obtained parameters are in good agreement with parameters obtained from Vogel-Fulcher fits, according to formula²⁶

$$T_0 = \Delta J/k_B. \quad (14)$$

We will discuss further below the obtained parameters together with random-bond random-field parameters of other mixed crystals.

D. Influence of small amount of selenium to phase-transition dynamics in CuInP_2S_6 crystals

Temperature dependence of the dielectric permittivity of CuInP_2S_6 crystals with a small amount of selenium ($x=0.98$) is presented in Fig. 10. A small amount of selenium changes dielectric properties of CuInP_2S_6 crystals significantly: the temperature of the main dielectric anomaly shifts from about 315 to 289 K, the maximum value of the dielectric permittivity ϵ' significantly decreases from about 180 to 40 (at 1 MHz), at higher frequencies (from about 10 MHz) the peak of dielectric permittivity becomes frequency dependent in $\text{CuInP}_2(\text{S}_{0.98}\text{Se}_{0.02})_6$ crystals, and a critical slowing down disappears.⁶ An additional dielectric dispersion appears at low frequencies and at low temperatures. The $\text{CuInP}_2(\text{S}_{0.95}\text{Se}_{0.05})_6$ crystals exhibit qualitatively similar dielectric anomaly with T_c and ϵ'_{max} shifting to lower values. The dielectric dispersion of presented crystals is symmetric

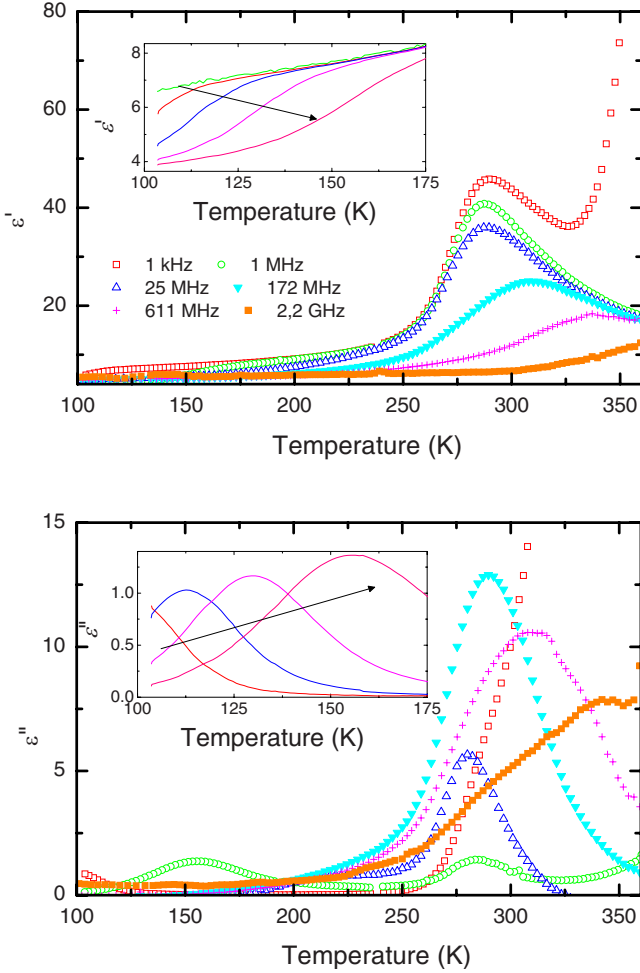


FIG. 10. (Color online) Temperature dependence of the complex dielectric permittivity of $\text{CuInP}_2(\text{S}_{0.98}\text{Se}_{0.02})_6$ crystals measured at several frequencies.

so that it can be correctly described by the Cole-Cole formula [Eq. (1)]. The Cole-Cole parameters are shown in Fig. 11. The parameters of the Cole-Cole distribution of relaxation α_{CC} strongly increase on cooling and reach 0.43 at low temperatures. The temperature dependence of the dielectric strength $\Delta\varepsilon$ was fitted with the Curie-Weiss law [Eq. (2)]. Obtained parameters are summarized in Table IV. The difference $T_{C_p} - T_{C_f}$ and ratio C_p/C_f in these crystals indicate a first-order, order-disorder phase transition. In ferroelectric phase the mean relaxation time τ_{CC} decreases only in a narrow temperature region and only for $\text{CuInP}_2(\text{S}_{0.98}\text{Se}_{0.02})_6$, further on cooling a significant increasing of time τ_{CC} is observed. This increasing can be easily explained by the Fogel-Vulcher law [Eq. (7)]. These parameters are summarized in Table V. Note that all parameters of different compounds in Table V are close to each other. Such a behavior is very similar to behavior of betaine phosphite with a small amount of betaine phosphate²⁷ and in $\text{Rb}_{1-x}(\text{NH}_4)_x\text{H}_2\text{AsO}_4$ (RADA) (Ref. 28) crystals, where a proposition that a coexistence of the ferroelectric order and dipolar glass disorder appears at low temperatures was proposed. Therefore we can conclude that mixed $\text{CuInP}_2(\text{S}_x\text{Se}_{1-x})_6$ crystals with $x \geq 0.95$ also exhibit a coexistence of ferroelectric and dipolar glass disorder at low temperatures.

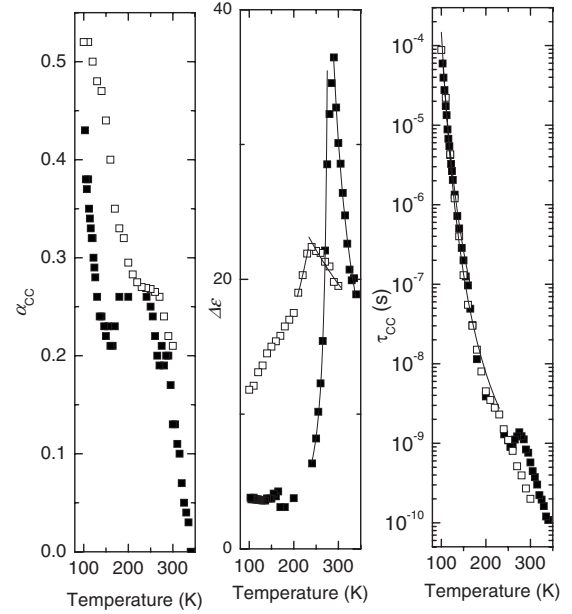


FIG. 11. Temperature dependence of the Cole-Cole parameters of complex dielectric permittivity for the $\text{CuInP}_2(\text{S}_x\text{Se}_{1-x})_6$ crystals with $x=0.95$ (open points) and $x=0.98$ (solid points). The τ lines were obtained from Vogel-Fulcher fit and the $\Delta\varepsilon$ lines were obtained from Curie-Weiss fit.

E. Phase diagram

In this section we will discuss phase diagram in terms of random bonds and random fields. For ferroelectrics we assume that mean coupling constant J/k is equal to T_C because Curie-Weiss fit is accurate for these compounds and in this case Eq. (9) becomes Curie-Weiss law. Also for crystals with $x \leq 0.1$, for the same reason we assume that ΔJ and Δf are 0. For ferroelectrics with $x \geq 0.95$ we obtained ΔJ from T_0 [Eq. (14)], and we assumed that $\Delta f = 0$.

In Fig. 12 we present the obtained phase diagram of mixed crystals. In the mixed $\text{CuInP}_2(\text{S}_x\text{Se}_{1-x})_6$ with $x \geq 0.95$ and $x \leq 0.1$ crystals the mean coupling constant $J > (\Delta f + \Delta J^2)^{0.5}$, therefore, undergo ferroelectric phase transition at J/k . However, it is a significant difference between phase-transition dynamics of mixed crystals with $x \geq 0.95$ and $x \leq 0.1$. In mixed crystals with $x \leq 0.1$ no any coexistence of ferroelectric order and dipolar glass disorder is observed down to the lowest temperature (80 K). At temperatures below 100 K the dielectric permittivity of these compounds is very low (about 3); therefore, the phase coexistence in these compounds is unlikely. In the ferroelectric phase these crystals split into domains; it is evidenced in

TABLE IV. Parameters of phase-transition dynamics of CuInP_2S_6 crystals with small admixture of selenium.

Compound	C_p (K)	C_p/C_f	T_{C_p} (K)	T_{C_f} (K)
$\text{CuInP}_2(\text{Se}_{0.05}\text{S}_{0.95})_6$	8587.7	2.99	137.2	368.7
$\text{CuInP}_2(\text{Se}_{0.02}\text{S}_{0.98})_6$	1906.5	7.01	236.9	282.6

TABLE V. Parameters of the Vogel-Fulcher fit of the temperature dependencies of the mean relaxation times τ_{CC} in $\text{CuInP}_2(\text{S}_x\text{Se}_{1-x})_6$ inhomogeneous ferroelectrics.

Compound	τ_0 (s)	T_0 (K)	E/k (K)
$\text{CuInP}_2(\text{Se}_{0.95}\text{S}_{0.05})_6$	8.5×10^{-12}	1150	31
$\text{CuInP}_2(\text{Se}_{0.98}\text{S}_{0.02})_6$	3.77×10^{-11}	1215	28

low-frequency dielectric dispersion spectra (Fig. 1). However similar ferroelectric domains already are observed in pure $\text{CuInP}_2\text{Se}_6$ crystals.⁹ Really, influence of small amount of sulfur to phase-transition dynamics of mixed crystals appears only by reduction in T_C (Table I). The influence of small amount of selenium to phase-transition dynamics is more significant—already at $x=0.95$ the ferroelectric phase transition in τ_{CC} is less expressed (Fig. 11). Such influence is expressed also in other properties: rapid decrease in T_C , appearance of ferroelectric and dipolar glass phase coexistence at $x=0.98$, and onset of dipolar glass disorder with x between 0.9 and 0.95. For crystals with $x=0.2$ and 0.25, $J < (\Delta f + \Delta J^2)^{0.5}$ and $J \approx (\Delta f + \Delta J^2)^{0.5}$, therefore the nonergodic relaxor phase appears in these crystals at low temperatures. In the presence of an external electric field E meaning coupling constant J is expected to vary as

$$J(E) = J(0) + \alpha E^2. \quad (15)$$

For electrical field E that $J(E) > (\Delta f + \Delta J^2)^{0.5}$ and in mixed crystals should be observed relaxor to ferroelectric phase transition. The possible existence of relaxor phase in mixed ferroelectric-antiferroelectric crystals is stated in Refs. 13 and 29. Really, no any evidence is indicated for polar nanoregion existence in mixed crystals. We try to fill this gap of information presenting two mixed crystals, where dielectric behavior is very similar to very well-known relaxors PMN (Ref. 30) and SBN (Ref. 31) (the differences are only in T_m and ε'_{\max} values). On the other hand, in phase diagram with less selenium concentration no area with nonergodic relaxor phase (Fig. 12) appears. The main cause of such phase diagram is that disorder $[(\Delta f + \Delta J^2)^{0.5}]$ is the highest at $x=0.2$, where mean coupling constant is also high enough. Usually, for mixed crystals it is assumed that concentration dependence for Δf is such²⁴

$$\Delta f = 4x(1-x)\Delta f_{\max}. \quad (16)$$

For ΔJ^2 similar behavior also was assumed. In this case if J has minimum at $x=0.5$ the nonergodic relaxor phase cannot be observed. However any existing theories cannot explain ΔJ and Δf concentration dependences. For compounds $0.9 \geq x \geq 0.4$ the relation $J \ll (\Delta f + \Delta J^2)^{0.5}$ is valid; consequently in these compounds a dipolar glass phase appears at low temperatures.

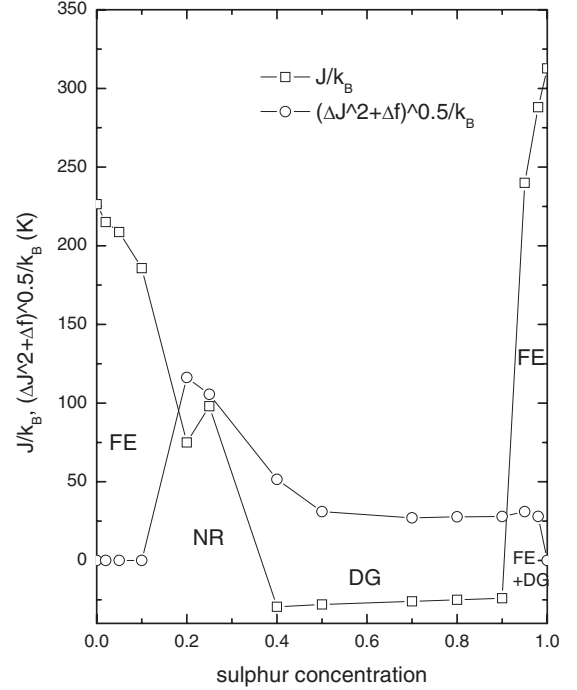


FIG. 12. Phase diagram of the mixed $\text{CuInP}_2(\text{S}_x\text{Se}_{1-x})_6$ crystals (FE—ferroelectric phase, NR—nonergodic relaxor phase, DG—dipolar glass phase, and FE+DG—ferroelectric and dipolar glass coexistence).

IV. CONCLUSIONS

The ferroelectric order in CuInP_2S_6 is reduced already for small ($x=0.98$) substitution of sulfur by selenium. By further increasing selenium concentration the dipolar glass phase appears. In contrast to $\text{CuInP}_2\text{Se}_6$ even a high concentration of admixture of sulfur ($x=0.1$) has no any influence to the ferroelectric order. Some degree of ferroelectric order exists even for $x=0.2$ and $x=0.25$; however, in these crystals the ferroelectricity is broken into polar nanoregions. The random-bond and random-field models clearly describe the asymmetry of phase diagram of mixed $\text{CuInP}_2(\text{S}_x\text{Se}_{1-x})_6$; however this model cannot identify the origin of the effect. To summarize, the first experimental evidence for smearing nonergodic relaxor phase into dipolar glass phase by some doping is presented. For other relaxors the search of some admixture which transforms relaxor state into dipolar glass can also be performed.

ACKNOWLEDGMENTS

We acknowledge useful conversations and technical assistance from G. Valusis, S. Lapinskas, and G. Voelkel. This work was performed under the auspices of the Lithuanian Science and Study Foundation and Lithuanian Ministry of Education and Science under the Lithuanian-Ukrainian projects.

*jan@pfi.lt

- ¹V. Maisonneuve, V. B. Cajipe, A. Simon, R. Von Der Muhll, and J. Ravez, Phys. Rev. B **56**, 10860 (1997).
- ²V. B. Cajipe, J. Ravez, V. Maisonneuve, A. Simon, C. Payen, R. Von Der Muhl, and J. E. Fischer, Ferroelectrics **185**, 135 (1996).
- ³X. Bourdon, A. R. Grimmer, and V. B. Cajipe, Chem. Mater. **11**, 2680 (1999).
- ⁴Yu. M. Vysochanskii, V. A. Stephanovich, A. A. Molnar, V. B. Cajipe, and X. Bourdon, Phys. Rev. B **58**, 9119 (1998).
- ⁵V. Maisonneuve, J. M. Reau, Ming Dong, V. B. Cajipe, C. Payen, and J. Ravez, Ferroelectrics **196**, 257 (1997).
- ⁶J. Banys, J. Macutkevic, V. Samulionis, A. Brilingas, and Yu. Vysochanskii, Phase Transitions **77**, 345 (2004).
- ⁷Yu. M. Vysochanskii, A. A. Molnar, M. I. Gurzan, V. B. Cajipe, and X. Bourdon, Solid State Commun. **115**, 13 (2000).
- ⁸X. Bourdon, V. Maisonneuve, V. B. Cajipe, C. Payen, and J. E. Fischer, J. Alloys Compd. **283**, 122 (1999).
- ⁹J. Banys, J. Macutkevic, and Yu. Vysochanskii, Phys. Status Solidi A (to be published).
- ¹⁰Yu. M. Vysochanskii, A. A. Molnar, V. A. Stephanovich, V. B. Cajipe, and X. Bourdon, Ferroelectrics **226**, 243 (1997).
- ¹¹Yu. M. Vysochanskii, A. A. Molnar, V. A. Stephanovich, V. B. Cajipe, and X. Bourdon, Ferroelectrics **257**, 147 (2001).
- ¹²J. Banys, R. Grigalaitis, J. Macutkevic, A. Brilingas, V. Samulionis, J. Grigas, and Yu. Vysochanskii, Ferroelectrics **318**, 163 (2005).
- ¹³E. Matsushita and K. Takahashi, Jpn. J. Appl. Phys., Part 1 **41**, 7184 (2002).
- ¹⁴A. N. Tikhonov and V. Y. Arsenin, *Solution of Ill-Posed Problems* (Wiley, New York, 1977).
- ¹⁵J. Banys, J. Macutkevic, S. Lapinskas, C. Klimm, G. Völkel, and A. Klöpperpieper, Phys. Rev. B **73**, 144202 (2006).
- ¹⁶R. Grigalaitis, J. Banys, A. Kania, and A. Slodczyk, J. Phys. IV **128**, 127 (2005).
- ¹⁷J. Macutkevic, S. Kamba, J. Banys, A. Brilingas, A. Pashkin, J. Petzelt, K. Bormanis, and A. Sternberg, Phys. Rev. B **74**, 104106 (2006).
- ¹⁸S. Kamba, D. Nuzhnyy, S. Veljko, V. Bovtun, J. Petzelt, Y. L. Wang, N. Setter, J. Levoska, M. Tyunina, J. Macutkevic, and J. Banys, J. Appl. Phys. **102**, 074106 (2007).
- ¹⁹J. Banys, J. Macutkevic, R. Grigalaitis, and W. Kleemann, Phys. Rev. B **72**, 024106 (2005).
- ²⁰R. Pirc, R. Blinc, and V. Bobnar, Phys. Rev. B **63**, 054203 (2001).
- ²¹R. Pirc and R. Blinc, Phys. Rev. B **76**, 020101(R) (2007).
- ²²R. Blinc, J. Dolinsek, A. Gregorovic, B. Zalar, C. Filipic, Z. Kutnjak, A. Levstik, and R. Pirc, Phys. Rev. Lett. **83**, 424 (1999).
- ²³Yu. Vysochanskii, L. Beley, S. Perechinskii, M. Gurzan, O. Molnar, O. Mykajlo, V. Tovt, and V. Stephanovich, Ferroelectrics **298**, 361 (2004).
- ²⁴R. Pirc, B. Tadic, and R. Blinc, Phys. Rev. B **36**, 8607 (1987).
- ²⁵J. M. B. Lopes dos Santos, M. L. Santos, M. R. Chaves, A. Almeida, and A. Klöpperpieper, Phys. Rev. B **61**, 8053 (2000).
- ²⁶R. Kind, R. Blinc, J. Dolinsek, N. Korner, B. Zalar, P. Cevc, N. S. Dalal, and J. DeLooze, Phys. Rev. B **43**, 2511 (1991).
- ²⁷J. Banys, J. Macutkevic, A. Brilingas, J. Grigas, C. Klimm, and G. Voelkel, Phase Transitions **78**, 869 (2005).
- ²⁸Z. Trybula, V. H. Schmidt, and J. E. Drumheller, Phys. Rev. B **43**, 1287 (1991).
- ²⁹N. Korner, Ch. Pfammatter, and R. Kind, Phys. Rev. Lett. **70**, 1283 (1993).
- ³⁰A. Levstik, Z. Kutnjak, C. Filipic, and R. Pirc, Phys. Rev. B **57**, 11204 (1998).
- ³¹W. Kleemann, J. Dec, S. Miga, Th. Woike, and R. Pankrath, Phys. Rev. B **65**, 220101(R) (2002).